

Bi-Arrhenius Diffusion and Surface Trapping of $^8\text{Li}^+$ in Rutile TiO_2

A. Chatzichristos^{1,2,*}, R. M. L. McFadden,^{2,3} M. H. Dehn,^{1,2} S. R. Dunsiger,⁴ D. Fujimoto,^{1,2} V. L. Karner,^{2,3}
 I. McKenzie,^{5,6} G. D. Morris,⁵ M. R. Pearson,⁵ M. Stachura,⁵ J. Sugiyama,^{7,8,9} J. O. Ticknor,^{2,3}
 W. A. MacFarlane,^{2,3,5} and R. F. Kiefl^{1,2,5,†}

¹Department of Physics and Astronomy, University of British Columbia, Vancouver, BC V6T 1Z1, Canada

²Stewart Blusson Quantum Matter Institute, University of British Columbia, Vancouver, BC V6T 1Z4, Canada

³Department of Chemistry, University of British Columbia, Vancouver, BC V6T 1Z4, Canada

⁴Department of Physics, Simon Fraser University, Burnaby, BC V5A 1S6, Canada


⁵TRIUMF, 4004 Wesbrook Mall, Vancouver, BC V6T 2A3, Canada

⁶Department of Chemistry, Simon Fraser University, Burnaby, BC V5A 1S6, Canada

⁷Toyota Central Research and Development Laboratories, Inc., Nagakute, Aichi 480-1192, Japan

⁸Advanced Science Research Center, Japan Atomic Energy Agency, Tokai, Ibaraki 319-1195, Japan

⁹CROSS Neutron Science and Technology Center, 162-1 Shirakata, Tokai, Naka, Ibaraki 319-1106, Japan

 (Received 4 March 2019; published 29 August 2019)

We report measurements of the diffusion rate of isolated ion-implanted $^8\text{Li}^+$ within ~ 120 nm of the surface of oriented single-crystal rutile TiO_2 using a radiotracer technique. The α particles from the ^8Li decay provide a sensitive monitor of the distance from the surface and how the depth profile of ^8Li evolves with time. The main findings are that the implanted Li^+ diffuses and traps at the (001) surface. The T dependence of the diffusivity is described by a bi-Arrhenius expression with activation energies of 0.3341 (21) eV above 200 K, whereas at lower temperatures it has a much smaller barrier of 0.0313(15) eV. We consider possible origins for the surface trapping, as well the nature of the low- T barrier.

DOI: 10.1103/PhysRevLett.123.095901

It is well known [1,2] that Li^+ diffusion in rutile TiO_2 through the c -axis channels is extremely fast, greatly surpassing all other interstitial cations [3], with a room temperature diffusion coefficient exceeding many modern solid-state Li electrolytes [4]. A major limitation to its use as an electrode material in Li-ion batteries is its limited Li uptake at room temperature [5,6]; however, the discovery that using nanosized crystallites mitigates this issue [7] has led to renewed interest in its applicability [8].

There are multiple poorly understood aspects of rutile lithiation, including the cause of the limited Li^+ uptake, or why reported Li diffusion rates differ by orders of magnitude under the same experimental conditions [1,9–13]. Theoretical studies (e.g., Refs. [14–20]) have been unable to reproduce the characteristics of Li^+ migration found in experiments [1,11,13]. A direct technique applicable to the nanoscale could help resolve these issues. To this end, we developed a variation to the classical radiotracer method, the ^8Li α -radiotracer method, which uses the attenuation of the progeny α particles from the radioactive decay of ^8Li to study Li diffusion. This method differs from conventional radiotracer diffusion experiments in several key aspects: (a) it is nondestructive, (b) it is sensitive to motions on the nanometer scale [21], (c) it is applicable to thin films and heterostructures, and (d) it is amenable for the use of short-lived isotopes ($\tau_{1/2} \sim 1$ s).

In this study, we employ the α -radiotracer method to extract the diffusion coefficient and its activation energy for isolated Li in rutile TiO_2 and show that Li^+ traps at the (001) rutile surface. Furthermore, we report that the nanoscale Li diffusion exhibits bi-Arrhenius behavior. The high- T (above ~ 200 K) activation energy and diffusion rate are in agreement with previous studies. The low- T behavior is discussed in the context of the recently reported Li- Ti^{3+} polaron complex [13]; here we suggest that part of that signal is connected to Li hopping or diffusion.

The experiment was performed using the ISAC facility at TRIUMF [22], in Vancouver, Canada. The samples were commercial chemomechanically polished (roughness < 0.5 nm) single-crystal rutile TiO_2 substrates (CRYSTAL-GmbH) with dimensions of $7 \times 7 \times 0.5$ mm³.

In the experiment, a 1 sec beam pulse of low energy (available range: 0.1–30 keV) $^8\text{Li}^+$ with an intensity of $\sim 10^6$ $^8\text{Li}^+$ /sec is implanted close to the surface of the rutile targets housed in an ultrahigh vacuum cold finger cryostat [22,23]. The beam energy defines the initial Li^+ implantation profile (see Fig. 1). Upon arrival, the $^8\text{Li}^+$ starts to diffuse through the sample and β decays to ^8Be , which then decays (immediately) into two α particles, each with a mean energy of 1.6 MeV and an energy distribution with an asymmetric high-energy tail [24]. Because of their rapid attenuation inside the sample, the highest energy α particles escaping the sample originate from $^8\text{Li}^+$ that have diffused back closer to the surface.

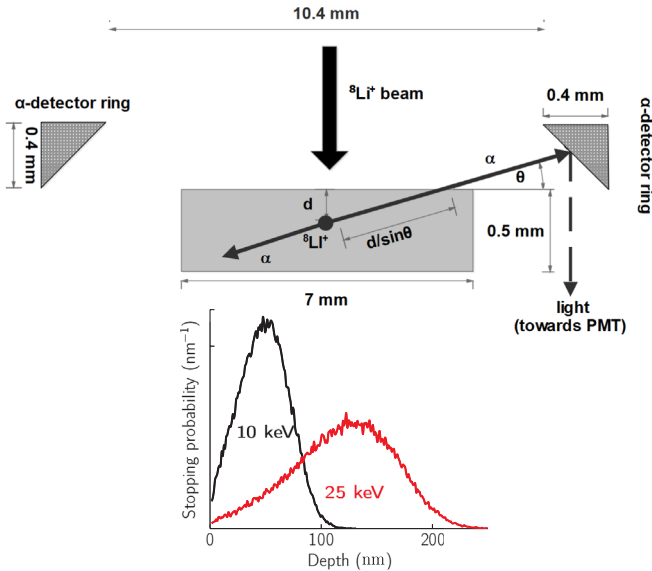


FIG. 1. *Top*: Schematic of the sample region showing the cross section of the ring detector. The α particles originating at depth d that reach the α -detector traverse distance $d/\sin\theta$ [25] through the sample. Not to scale. *Bottom*: Initial implantation profiles for beam energy of 10 and 25 keV as simulated by SRIM.

To further amplify the sensitivity to near-surface ${}^8\text{Li}^+$, the α detector is placed at a grazing angle, $\theta \leq 4.4^\circ$, relative to the surface (Fig. 1). The α detector in our setup is an Al ring, whose inside surface is cut at $\sim 45^\circ$ and coated with a thin layer of Ag-doped ZnS, a well-known scintillator sensitive to α particles [26]. The light output is collected in the forward direction using two lenses that focus the light onto the photocathode of a fast photomultiplier (PMT). The PMT pulses have a large signal-to-noise ratio (> 10) and pass through a timing filter amplifier to be discriminated, so that only the top 1/3 of pulses above the noise level are counted. This corresponds to an effective energy threshold of about 2 MeV.

The diffusion rate of Li inside the sample is directly related to the time it takes to reach the surface, which in turn relates to the α rate as a function of time, as the probability of detecting a high-energy α vs depth $P_{\text{det}}(d)$ drops steeply in the first ~ 100 nm, to about half its surface value at $d = 200$ nm. This method has intrinsic timescales and length scales of $\tau_{1/2} \sim 1$ s and $d \sim 100$ nm, which leads to a theoretical sensitivity to the diffusion rate D from 10^{-12} to 10^{-8} $\text{cm}^2 \text{s}^{-1}$. However, our effective sensitivity limit is closer to 10^{-11} $\text{cm}^2 \text{s}^{-1}$, determined by experimental factors such as the finite counting statistics and the existence of small distortions due to pileup in the detector response. In addition, the experimental sensitivity is somewhat better for a lower implantation energy (see Fig. 4).

When Li^+ is immobile, the probability of detecting an α for any given decay event is time independent and the measured α counts follow the decay rate of ${}^8\text{Li}$. This is

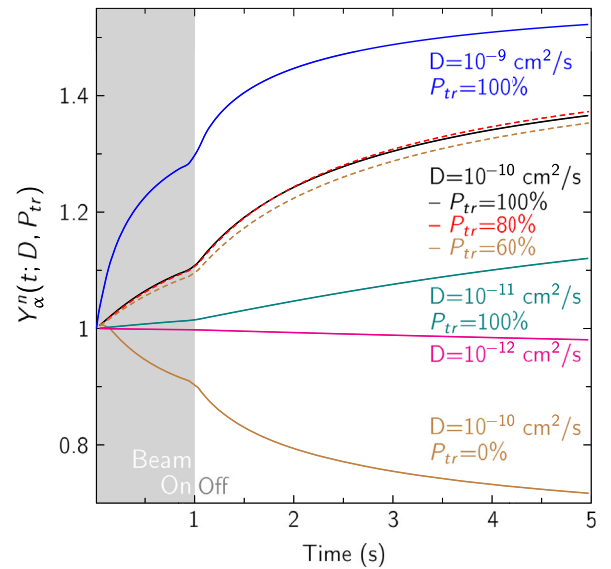


FIG. 2. Calculated normalized α -to- β ratio $[\bar{Y}_\alpha^n(t; D, P_{tr})]$ in TiO_2 , for an implantation time of 1 s, beam energy of 25 keV, and different values of D and P_{tr} . The time dependence of the signal is due to changes in the ${}^8\text{Li}^+$ depth profile due to diffusion.

monitored using the β particles from the ${}^8\text{Li}$ decay, which are weakly attenuated over these distances. Thus, the ratio of counts $Y_\alpha = N_\alpha/N_\beta$ are constant in time. On the other hand, when Li^+ is mobile, $Y_\alpha(t)$ is time dependent when the mean diffusion length in the ${}^8\text{Li}$ lifetime is comparable to the mean depth of implantation, reflecting the fact that the ${}^8\text{Li}^+$ depth distribution is evolving in time. The information on Li diffusion comes from the time evolution of the Y_α signal. The absolute α -to- β ratio, i.e., the *baseline* of Y_α in the absence of diffusion, depends on experimental factors such as detector efficiencies; therefore to account for these systematics, each α spectrum is self-normalized to start from unity at time zero, i.e., $Y_\alpha^n(t) = Y_\alpha(t)/Y_\alpha(0^+)$ [27].

In order to extract the Li diffusion rate, the experimentally acquired $Y_\alpha^n(t)$ was compared to a library of simulated $\bar{Y}_\alpha^n(t)$ signals. To this end, we performed numerical solutions to Fick's laws in one dimension to generate the time-evolved depth distribution of ${}^8\text{Li}^+$, accounting for the boundary conditions of the crystal surface and the initial ${}^8\text{Li}^+$ stopping profile as simulated by the SRIM Monte Carlo package [28] (inset in Fig. 1). $\bar{Y}_\alpha^n(t; D)$ is then obtained by multiplying each bin of the depth profile of ${}^8\text{Li}$ with $P_{\text{det}}(d)$. $P_{\text{det}}(d)$ was extracted using the GEANT4 [29] simulation package. In the simulations shown in Fig. 2 and also in the experimental data, the beam pulse is precisely set to 1 sec in duration. After that it is turned off for 19 sec to allow all the ${}^8\text{Li}$ to decay. The qualitative characteristics of $\bar{Y}_\alpha^n(t; D)$ were found to depend heavily on the probability of ${}^8\text{Li}^+$ trapping upon reaching the sample surface, P_{tr} (see Fig. 2), implying that one can infer the ${}^8\text{Li}^+$

behavior at the surface, i.e., whether it is primarily trapped or reflected.

When $P_{\text{tr}} \geq 50\%$ $\bar{Y}_\alpha^n(t; D, P_{\text{tr}})$ is nearly P_{tr} independent and faster diffusion results in a monotonically increasing $\bar{Y}_\alpha^n(t; D, P_{\text{tr}})$, while $P_{\text{tr}} < 20\%$ leads to $\bar{Y}_\alpha^n(t; D, P_{\text{tr}})$ that decreases with time, since the overall mean distance from the surface will increase with time as the Li primarily migrates away from the surface back to the bulk of the sample, towards the uniform depth distribution.

A technique similar to the one discussed here has been developed by Jeong *et al.* [30] for Li^+ diffusion on a micrometer and, recently, by Ishiyama *et al.* [21] on nanometer length scales; however, this experiment differs in a few key ways. In particular, the ^8Li implantation rates accessible at TRIUMF (typically 10^6 – 10^7 $^8\text{Li}^+/\text{s}$) are 1–2 orders of magnitude larger [21], which allows the α detector to be placed at a grazing angle $\theta [\leq 4.4^\circ$ vs $10(1)^\circ$ [27]]. This detector configuration significantly decreases the α counts, but greatly enhances the sensitivity to the near-surface region. In addition, the ZnS:Ag ring detector used in the present setup is much simpler and easier to install close to the sample in UHV compared to a Si detector [27], although it has less energy resolution.

Here we report α -radiotracer measurements on rutile TiO_2 at various temperatures with two beam energies (10 and 25 keV) and two sample orientations. As Li^+ is known to diffuse primarily along the c axis of rutile, for the (110)-orientation (c axis parallel to the surface), the $^8\text{Li}^+$ motion should not change the initial implantation profile. Since the ab -plane diffusivity $D_{ab} \ll 10^{-12} \text{ cm}^2 \text{ s}^{-1}$, $Y_\alpha^n(t)$ is expected to be time independent. On the other hand, for the (001) orientation (c axis normal to the surface), the depth distribution of lithium should be evolving with time, since $D_c \gg 10^{-12} \text{ cm}^2 \text{ s}^{-1}$.

In Fig. 3 we compare the measured normalized α yield Y_α^n for the two orientations. As expected for the (110) orientation, $Y_\alpha^n(t)$ is completely flat at 294 K, indicating that the ab -plane diffusion rate is lower than the theoretical detection limit $\sim 10^{-12} \text{ cm}^2 \text{ s}^{-1}$, consistent with other studies reporting a $D_{ab} \leq 10^{-15} \text{ cm}^2 \text{ s}^{-1}$ [1]. Also shown in Fig. 3 are examples of experimental data for the (001) orientation in the range of 60 to 370 K, with the corresponding fits to the model described above.

To fit the data, we used a custom C++ code applying the MINUIT [31] minimization functionalities of ROOT [32] to compare the Y_α^n signals to the library of calculated spectra \bar{Y}_α^n . The free parameters of the fit were D and P_{tr} . All $Y_\alpha^n(t; D, P_{\text{tr}})$ spectra at both implantation energies (10 and 25 keV) were fitted simultaneously with a shared P_{tr} value. For the (001)-orientation $Y_\alpha^n(t)$ increases rapidly, approaching saturation, indicating that lithium diffuses fast along the c axis and gets trapped at (or within few nm of) the surface (see Fig. 2). For $P_{\text{tr}} \geq 50\%$, the global χ^2 value is completely insensitive to P_{tr} , but for $P_{\text{tr}} < 50\%$, the quality of the fits deteriorates rapidly.

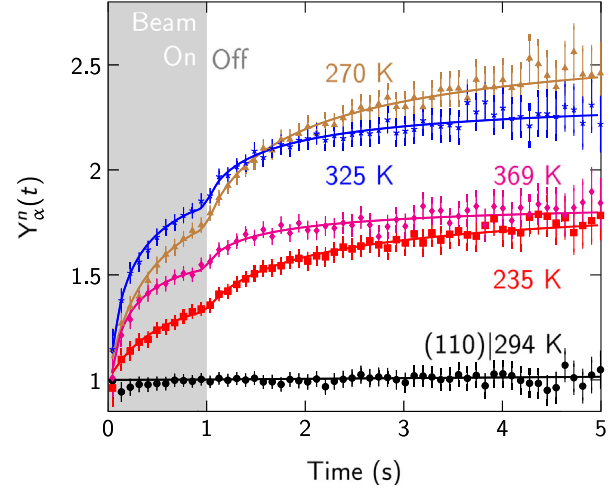


FIG. 3. Example spectra showing the measured α -to- β ratio [$Y_\alpha^n(t)$] from ^8Li implanted in rutile at a few representative temperatures. The beam energy in the spectra shown here was 25 keV. The beam pulse is 1 sec after which the beam is turned off for 19 sec. All data shown are for a (001)-oriented rutile crystal, except for the bottom (black circles), which is for the (110) orientation. The fitted curves are fits to a diffusion model assuming the $^8\text{Li}^+$ traps with trapping probability $P_{\text{tr}} = 100\%$ at the surface (see text). In the (001) crystal, $Y_\alpha^n(t; D)$ saturates more rapidly for increasing temperature, indicating that above room temperature, most of the Li gets trapped at the (001) surface during its lifetime. Above room temperature, $Y_\alpha^n(t; T)$ get progressively suppressed, as the normalization factor $Y_\alpha(t = 0^+; T)$ increases substantially due to the very fast diffusion.

To understand this, one can see in Fig. 2 how similar the signals are for $P_{\text{tr}} = 100$ and 60% for the same D . This is the first *unambiguous* evidence for Li trapping (with at least 50% probability) at the (001) surface. There is no evidence of Li detrapping up to 370 K, since at that temperature $Y_\alpha^n(t; T)$ reaches saturation after ~ 2 s and any Li surface detrapping would lead to an observable decrease of $Y_\alpha^n(t; T)$ at later times. The high trapping probability is most likely related to the difficulty of Li intercalation, as Li^+ would tend to stick at or near the surface rather than diffusing into the bulk.

It is not clear whether the Li^+ surface trapping is caused by an electrostatic potential well [33], a partially reconstructed surface [34], or by a chemical sink either due to an adsorbate, or a solid state reaction at the surface (e.g., forming cubic LiTiO_2). Subsequent measurements of an adsorbate-free rutile sample, as well as samples capped with thin layers of materials capable of altering the surface chemistry are needed to resolve this question.

Turning to the values of $D(T)$ extracted using the above analysis (see Fig. 4), they reveal a bi-Arrhenius relationship of the form

$$D(T) = D_H \exp[-E_H/(k_B T)] + D_L \exp[-E_L/(k_B T)], \quad (1)$$

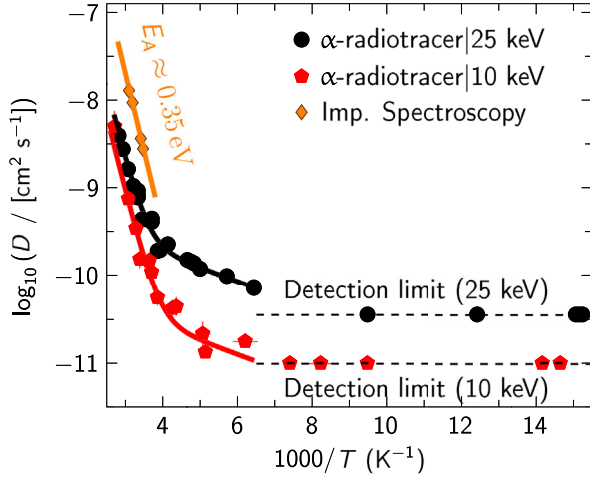


FIG. 4. Arrhenius plot, comparing reported Li diffusion rates in rutile TiO_2 [11,13]. The solid black and red lines are the bi-Arrhenius fits of Eq. (1) with $P_{\text{tr}} = 100\%$. For comparison we also show results using impedance spectroscopy [11].

where E_i is the activation energy and D_i is the prefactor of each component. These yielded $E_H = 0.3341(21)$ eV and $D_H = 2.31(18) \times 10^{-4}$ $\text{cm}^2 \text{s}^{-1}$ for the high- T component and $E_L = 0.0313(15)$ eV and $D_L = 7.7(7) \times 10^{-10}$ $\text{cm}^2 \text{s}^{-1}$ for the low- T component. E_H is in excellent agreement with values deduced by other techniques [1,11,13] and the diffusion rates at high T are lower by a factor of ~ 10 compared to the ones found using impedance spectroscopy [11]. However, this difference is not unexpected given the two methods have different systematics. For example, our measurements are on single crystals whereas the impedance spectroscopy is done on nanorods. Also, we are looking at $^8\text{Li}^+$ diffusion, which is slightly heavier than stable Li.

Both datasets (beam energies of 10 and 25 keV) yield virtually the same bi-Arrhenius activation energies and they are in agreement at high T , but the low- T component of the 10 keV data is shifted lower by about an order of magnitude. For trapping probability $P_{\text{tr}} < 100\%$, the apparent gap narrows but persists even for P_{tr} as small as 50%. One possibility is that there is a discrepancy between the SRIM and the actual implantation profiles, possibly due to channeling [35]. However, a measurement with the sample tilted by 10° revealed no significant difference in the signal. Another possibility is that there is some small random disorder close to the surface parametrized by some energy scale (Δ). At higher temperatures when $kT \gg \Delta$ its effect would diminish. This would explain why there is agreement between the two datasets at high temperatures but not so good at lower temperatures.

A bi-Arrhenius relationship for diffusivity is not uncommon; in vacancy ion conductors [36], it may occur from a crossover between a region where vacancies are thermally generated, to a region at lower T with a shallower slope. As an α radiotracer is only measuring the diffusion of Li^+ , rather than the net ionic conductivity, the origin of the two

Arrhenius components cannot be the same as above. While we cannot be conclusive about it, we consider some possibilities.

We first consider a recent β -NMR experiment on rutile [13], which also used an implanted $^8\text{Li}^+$ beam on similar crystals. The β -NMR measurements revealed two peaks in the relaxation rate $1/T_1$, one below 100 K and one above 200 K. Below 100 K, a 0.027 eV barrier was attributed to dynamics of electron polarons in the vicinity of the implanted ion [37,38]. In principle, these dynamics might not involve diffusion, e.g., if the $^8\text{Li}^+$ is static and the polaron is thermally trapped by the Li and cycles through trapping and detrapping. Nonetheless, our current measurement shows that there is some long-range diffusion of $^8\text{Li}^+$ at low T . While our E_L is comparable to that found with β -NMR, it is also compatible with the barrier predicted from theory for isolated Li in rutile [14–20,39]. The α radiotracer cannot distinguish whether Li moves either as a simple interstitial, or as part of a Li-polaron complex; it would only identify their weighted average contribution to the motion of $^8\text{Li}^+$. The similarity of the observed activation energy at low temperatures to the theoretical value suggests that a small fraction of the Li^+ interstitials does not combine with a polaron, but rather diffuses as a simple ion. If this fraction is small, that would explain why D_L is so much smaller than D_H .

It seems possible that the larger activation energy observed above 200 K may involve diffusion of a more complex object, possibly a Li-polaron complex, or it could be related to a disassociation energy of Li^+ with the polaron. Indeed, theory predicts a diffusion barrier of 0.29 eV for the Li-polaron complex and a disassociation energy of 0.45 eV [37], both comparable to the high- T barrier. The Li-polaron complex is electrically neutral, so its movement should contribute to the diffusivity of Li but not to the ionic conductivity. An electric field would not cause it to move—unless the potential gradient was strong enough to destabilize the complex. Thus, if it is a neutral Li-polaron complex moving at high T , one would expect the impedance measurement to yield a very different Arrhenius slope.

The much larger prefactor above 200 K, compared to low T is further evidence that these are two very different mechanisms for Li diffusion in rutile. Indeed, D_H , when written in terms of frequency, yields $\tau_H^{-1} \sim 2 \times 10^{12}$ s^{-1} , which is in the 10^{12} – 10^{13} s^{-1} range one would normally expect from phonons driving a thermally activated motion. Note that this frequency is ~ 5000 times smaller than what was found with β -NMR [13], as well as with optical absorption [1], which infer D indirectly, whereas this is a direct measurement.

In summary, we used the ^8Li α decay to study Li diffusion in a single-crystal rutile TiO_2 between 60 and 370 K. The diffusion rate was found to exhibit bi-Arrhenius behavior. We report a high- T activation energy $E_H = 0.3341(21)$ eV, in

agreement with other studies [1,11,13]. At low T , a second Arrhenius component was revealed, with an activation energy $E_L = 0.0313(15)$ eV. We suggest that this might be related to a small fraction of Li^+ that does not bind to a Li-polaron complex but rather hops as a simple interstitial with an activation energy near theoretical calculations. In addition, we found evidence that Li traps at the (001) surface, which could contribute to the reduced Li uptake at room temperature. We believe that this technique can shed new light on the Li motion in Li-ion battery materials and across their interfaces.

Special thanks to R. Abasalti, D. Vyas, and M. McLay for all their excellent technical support. This work was supported by: NSERC Discovery Grants to R. F. K. and W. A. M.; J. S. was supported by Japan Society for the Promotion Science (JSPS) KAKENHI Grant No. JP18H01863; and IsoSiM fellowships to A. C. and R. M. L. M. TRIUMF receives federal funding via a contribution agreement with the National Research Council of Canada.

* aris.chatzichristos@alumni.ubc.ca

† kiefl@triumf.ca

- [1] O. W. Johnson, *Phys. Rev.* **136**, A284 (1964).
- [2] O. W. Johnson and H. R. Krouse, *J. Appl. Phys.* **37**, 668 (1966).
- [3] J. A. Van Orman and K. L. Crispin, *Rev. Mineral. Geochem.* **72**, 757 (2010).
- [4] J. C. Bachman, S. Muy, A. Grimaud, H.-H. Chang, N. Pour, S. F. Lux, O. Paschos, F. Maglia, S. Lupart, P. Lamp, L. Giordano, and Y. Shao-Horn, *Chem. Rev.* **116**, 140 (2016).
- [5] D. W. Murphy, R. J. Cava, S. M. Zahurak, and A. Santoro, *Solid State Ionics* **9–10**, 413 (1983).
- [6] B. Zachau-Christiansen, K. West, T. Jacobsen, and S. Atlung, *Solid State Ionics* **28–30**, 1176 (1988).
- [7] Y.-S. Hu, L. Kienle, Y.-G. Guo, and J. Maier, *Adv. Mater.* **18**, 1421 (2006).
- [8] M. V. Reddy, G. V. Subba Rao, and B. V. R. Chowdari, *Chem. Rev.* **113**, 5364 (2013).
- [9] K. Kanamura, K. Yuasa, and Z. Takehara, *J. Power Sources* **20**, 127 (1987).
- [10] A. V. Churikov, V. A. Zobenkova, and K. I. Pridatko, *Russ. J. Electrochem.* **40**, 63 (2004).
- [11] S. Bach, J. P. Pereira-Ramos, and P. Willman, *Electrochim. Acta* **55**, 4952 (2010).
- [12] A. V. Churikov, A. V. Ivanishchev, A. V. Ushakov, and V. O. Romanova, *J. Solid State Electrochem.* **18**, 1425 (2014).
- [13] R. M. L. McFadden *et al.*, *Chem. Mater.* **29**, 10187 (2017).
- [14] M. V. Koudriachova, N. M. Harrison, and S. W. de Leeuw, *Phys. Rev. B* **65**, 235423 (2002).
- [15] F. Gligor and S. W. de Leeuw, *Solid State Ionics* **177**, 2741 (2006).
- [16] S. Kerisit, K. M. Rosso, Z. Yang, and J. Liu, *J. Phys. Chem. C* **113**, 20998 (2009).
- [17] H. Yildirim, J. P. Greeley, and S. K. R. S. Sankaranarayanan, *Phys. Chem. Chem. Phys.* **14**, 4565 (2012).
- [18] S. Kerisit, A. M. Chaka, T. C. Droubay, and E. S. Ilton, *J. Phys. Chem. C* **118**, 24231 (2014).
- [19] J. Jung, M. Cho, and M. Zhou, *AIP Adv.* **4**, 017104 (2014).
- [20] C. Arrouvel, T. C. Peixoto, M. E. G. Valerio, and S. C. Parker, *Comput. Theor. Chem.* **1072**, 43 (2015).
- [21] H. Ishiyama, S. C. Jeong, Y. X. Watanabe, Y. Hirayama, N. Imai, H. S. Jung, H. Miyatake, M. Oyaizu, A. Osa, Y. Otokawa, M. Matsuda, K. Nishio, H. Makii, T. K. Sato, N. Kuwata, J. Kawamura, H. Ueno, Y. H. Kim, S. Kimura, and M. Mukai, *Nucl. Instrum. Methods Phys. Res., Sect. B* **376**, 379 (2016).
- [22] G. D. Morris, *Hyperfine Interact.* **225**, 173 (2014).
- [23] Z. Salman, E. P. Reynard, W. A. MacFarlane, K. H. Chow, J. Chakhalian, S. R. Kreitzman, S. Daviel, C. D. P. Levy, R. Poutissou, and R. F. Kiefl, *Phys. Rev. B* **70**, 104404 (2004).
- [24] C. Forssén, E. Caurier, and P. Navrátil, *Phys. Rev. C* **79**, 021303(R) (2009).
- [25] H. Ishiyama, S.-C. Jeong, Y. Watanabe, Y. Hirayama, N. Imai, H. Miyatake, M. Oyaizu, I. Katayama, M. Sataka, A. Osa, Y. Otokawa, M. Matsuda, and H. Makii, *Jpn. J. Appl. Phys.* **52**, 010205 (2013).
- [26] T. Asada, M. Masuda, M. Okumura, and J. Okuma, *J. Phys. Soc. Jpn.* **14**, 1766 (1959).
- [27] H. Ishiyama, S. C. Jeong, Y. X. Watanabe, Y. Hirayama, N. Imai, H. Miyatake, M. Oyaizu, A. Osa, Y. Otokawa, M. Matsuda, K. Nishio, H. Makii, T. K. Sato, N. Kuwata, J. Kawamura, A. Nakao, H. Ueno, Y. H. Kim, S. Kimura, and M. Mukai, *Nucl. Instrum. Methods Phys. Res., Sect. B* **354**, 297 (2015).
- [28] J. F. Ziegler, M. D. Ziegler, and J. P. Biersack, *Nucl. Instrum. Methods Phys. Res., Sect. B* **268**, 1818 (2010).
- [29] J. Allison *et al.*, *Nucl. Instrum. Methods Phys. Res., Sect. A* **835**, 186 (2016).
- [30] S.-C. Jeong *et al.*, *Nucl. Instrum. Methods Phys. Res., Sect. B* **230**, 596 (2005).
- [31] F. James and M. Roos, *Comput. Phys. Commun.* **10**, 343 (1975).
- [32] R. Brun and F. Rademakers, *Nucl. Instrum. Methods Phys. Res., Sect. A* **389**, 81 (1997).
- [33] H. Okuyama, W. Siga, N. Takagi, M. Nishijima, and T. Aruga, *Surf. Sci.* **401**, 344 (1998).
- [34] U. Diebold, *Surf. Sci. Rep.* **48**, 53 (2003).
- [35] T. Beals, R. Kiefl, W. MacFarlane, K. Nichol, G. Morris, C. Levy, S. Kreitzman, R. Poutissou, S. Daviel, R. Baartman, and K. Chow, *Physica (Amsterdam)* **326B**, 205 (2003).
- [36] I. E. Hooton and P. W. M. Jacobs, *Can. J. Chem.* **66**, 830 (1988).
- [37] S. Kerisit, K. M. Rosso, Z. Yang, and J. Liu, *J. Phys. Chem. C* **113**, 20998 (2009).
- [38] A. T. Brant, N. C. Giles, and L. E. Halliburton, *J. Appl. Phys.* **113**, 053712 (2013).
- [39] M. V. Koudriachova, N. M. Harrison, and S. W. de Leeuw, *Phys. Rev. Lett.* **86**, 1275 (2001).